International Journal of Emerging Technology and Advanced Engineering
Website: www.ijetae.com (ISSN 2250-2459, ISO 9001:2008 Certified Journal, Volume 7, Issue 5, May 2017)

Design, Realization and Optimisation of A Flat-Plate Solar Collector for an Indirect Dryer of Cocoa Beans

Aka S. Koffi[1], N'Goran Yao[2], Kouakou Konan[3], Joseph K. Saraka[4], Denis Bruneau[5]

[1]PhD. Scholar,[2]Doctor « Énergie et Innovation Technologique » (EnIT) Laboratory of Physics of Condensed Matter and Technology, UFR Sciences of the Structures of Matter and Technology, Félix Houphouët-Boigny University of Cocody 22 B P 582, Abidjan, Côte d'Ivoire.

[3,4]Doctor, Electricité et conversion d'énergie » (ECEn), Institut National polytechnique Félix Houphouet-Boigny, Côte d'Ivoire.

[5]I2M -UMR 5295-, department TREFLE, University of Bordeaux, 33405 Talence Cedex, France.

***Abstract*— This article presents the performance of a thermal collector manufactured to transmit thermal energy to an indirect dryer of cocoa beans. The characteristics of the air at the outlet of the collector are, a maximum temperature about 46°C, a mean humidity of 46%, a air velocity mean 0.4 m/s and a low water vapour mass about 13 g/kg. These conditions are perfect for drying beans, and they are obtained at 15° for tilt angle value and at an elevation of 20 cm from the floor. The homogeneity of the temperature in the direction of the width of the collector makes it possible to improve its efficiency.**

***Keywords*—cocoa, collector efficiency, solar drying, tilt angle.**

I. Introduction

Cocoa beans (Theobroma cocoa L) are mainly used for the manufacture of chocolates [1]. After harvesting, the pods containing them are opened and the beans are collected for fermentation. During this process two chemical modifications take place in the bean, and permit the apparition of precursors of the chocolate flavor [2]. But at the end of fermentation there is water and acid (mainly acetic acid and acid lactic) in beans. The next phase is the drying, its permit to remove water and acid and also improves the quality of the beans by fixing the flavours formed previously and facilitating the storage. These two processes take place on the farm. Drying is therefore a key process for beans to have added value. It can be done mechanically by pressing, or chemically with silica gel or else thermally by boiling or with a circulation of hot air. The latter method is used more in agroprocessing and consists in putting the product in an hot and dry environment to permit a difference of temperature and partial pressure of water between both of them. This situation causes two types of spontaneous exchange for a gradual reduction of the solvents present in the bean. The first is the assimilation of heat from the environment and the second is release into this environment of solvents in vapor form [3], this is called dehydration [4].

The two major elements of this process are the heat source and the means used to deliver its energy to the product. For applications on agricultural products with low added value the commonly used and profitable energy source is the sun. Traditional techniques have the disadvantage of subjecting the beans to uncontrollable temperatures, exposing them to waste (plant and animal debris), and the resumption of moisture during the night [5]. In order to improve drying, the beans were physically isolated from the environment, with the introduction of 3 solar drying modes. In each mode there is a solar thermal collector for the production of heat and a drying chamber. The first is direct mode. In this mode the drying chamber is combined with the collector, so all surface below the transparent surface constitutes the drying area. Here the risk of exposing the beans to very high temperatures and thus preventing the enzymatic reactions is very great, of more the risk of trapping acidity in beans is even greater [6]. Moreover, in case of damage on the transparent surface the beans are immediately unprotected. The second is the indirect mode, where the two components are separated, and isolation is important in each part. Several drying racks can be used and the product is protected from unexpected sunburn. The last mode is the mixed, it is the combination of the two previous modes. This last is what we use.

To improve the performance of the collectors, they can be equipped with trackers to maximize the radiation captured [7] Or also a determination of the ideal angle of inclination from the geographical coordinates [8]. But tracker used was not yet popularized in agriculture and requires using of electrical equipment (like a motor) GPS coordinates are not always accessible by the producers, because more expansive. From this point of view, we decided to integrate into the collector design the changing of inclination and the relative height of the collector from the floor, as well as the limitation of the temperature and speed of the air at the outlet.

International Journal of Emerging Technology and Advanced Engineering
Website: www.ijetae.com (ISSN 2250-2459, ISO 9001:2008 Certified Journal, Volume 7, Issue 5, May 2017)

The aim of this study is to build a collector, which provides ideal conditions (temperature, humidity, air velocity) for the drying of an amount of about 20 kg of cocoa bean.

II. THEORICAL FRAMEWORK

A. Useful energy for sample drying

The energy produced by the collector is used to reduce cocoa beans moisture from 55% (W0) in wet base to a level, which is safe for storage, and shipment; that is 7.5% (W1) in wet base [9], [10]. Thus on 20 kg (M1) of beans, the quantity of water to be extracted (Me) will be calculated [3]

$$M_e = \frac{W_0 - W_1}{100 - W_1} M_1, \qquad (1)$$

The objective is to dry it on 24 h, this allow to calculate the drying speed:

$$V_{em} = \frac{M_e}{t_s}, \qquad (2)$$

To extract this quantity of water at this speed, it is necessary to provide a flow of hot air:

$$D_a = 1000 \frac{M_e}{t_s * \rho_{air} * \eta_s * (X_m - X_a)} \qquad (3)$$

In this equation ηs is the drying efficiency and empirically is taken to be equal to 0.5 to take account of losses in the flow rate, thus having a margin of safety. Xm is the mass of water vapor in ambient air. Xa is the mass of water vapor exhaust to collector. Xm et Xa are determined numerically [11] or graphically with the humid air pattern and expressed in kg / kg dry air in dry base. Finally, the power (P_n in W) of the collector for achieving this drying objective can be written in the following form:

$$P_n = \frac{\rho_{air} * C_{p\ air\ a} * (T_{s\ col} - T_{e\ col}) * D_a}{3600}, \qquad (4)$$

This equation depends on the density (ρ_{air}) of the air, the heat capacity ($C_{p\ air\ a}$) of the air, the temperature variation between the air at the collector outlet ($T_{s\ col}$) and that at the entrance ($T_{e\ col}$). The air flow calculated in (3) is also taken into account.

B. The collector size for energy production

To produce the power expressed by equation (4), we will need a collector with a surface area (in m²), it can be calculated as:

$$S_{col} = \frac{P_n}{\eta_c * \frac{G}{d_{in}}}, \qquad (5)$$

η_c is the collector efficiency, in order to take account of possible losses its value is carefully chosen, we opted for 0.33; G represents the total daily irradiation (3.27 kWh / m²) and d_{in} is the mean duration of sunshine (6.5 h). We deduced in meter (m) the length (L_{col}) and the width (ℓ_{col}) with:

$$S_{col} = L_{col} * \ell_{col} \qquad (6)$$

In order to take account of the speed limit of the air on the product, we include it in the determination of the height of the collector [12]

$$h_{col} = \frac{D_a}{3600 * v_{air\ s\ col} * L_{col}}, \qquad (7)$$

C. Solar collector efficiency

The collector realized in this study is double passage (Fig. 1); the power produced is the sum of the energies produced in each channel [13]. In each channel the usable power (in W) is calculated with the same formula, only the difference of temperature between the input and the output of the collector is linked to the channel and the air velocity in the channel. This speed is supposed to be uniform in each channel. For upper channel the power as calculated with the next relation: (8)

$$p_{n\ sup} = \frac{h_{col}}{2} * v_{air\ e\ col} * \rho_{air\ e\ col} * C_{p\ air\ a} * (T_{s\ col\ sup} - T_{e\ col\ sup}) \qquad (8)$$

$\frac{h_{col}}{2}$ is the height of the channel, because the absorber is at the middle height of the collector. The temperature at the inlet of each channel is considered different from the ambient temperature. The power received on the collector is considered the same for each channel, and is calculated as :

$$p_f = G_i * S_{col}, \qquad (9)$$

In this equation G_i is the instantaneous solar radiation (W / m²).

In equation (4) and (8) the heat capacity and density of air can be determined by [14]:

$$C_{p\ air\ a} = 1005{,}7 + 0{,}066(T - 27), \qquad (10)$$

$$\rho_{air\ e\ col} = 1{,}1774 - 0{,}00359(T - 27), \qquad (11)$$

Temperatures are in degrees Celsius (°C). Thus, the efficiency of the collector can be calculated by using:

$$\eta = \eta_{sup} + \eta_{inf} = \frac{p_{n\ sup}}{p_f} + \frac{p_{n\ inf}}{p_f}, \qquad (12)$$

Drying is also impacted directly by the mass of water vapor contained in 1 kg of air exhaust the collector, this quantity being determined with :

$$W_\infty = \frac{0{,}622 * P_{sat} * HR_\infty}{10132500 - (p_{sat} * HR_\infty)}, \qquad (13)$$

HR_∞ is the relative humidity of the air that is measured directly. P_{sat} is the partial pressure of the water vapor at saturation in mm Hg and is calculated with the following relationships according to the value of the air temperature T_∞:

if $T_\infty > 45°C$ $P_{sat} = \exp(23{,}1964 - \frac{3816{,}44}{T_\infty + 227{,}05})$,

(14)

if $0°C < T_\infty < 45°C$

$$P_{sat} = \exp[23{,}1964 - \frac{3802{,}7}{T_\infty + 273{,}18} - (\exp\frac{472{,}68}{T_\infty + 273{,}18})^2)],$$

(15)

III. Material

A. Experimental site

The experiments took place in southern of Côte d'Ivoire, in M'Brimbo on the Agricultural Society of Bandama (SAB). The coordinates of the collector location are for latitude 6 ° 02 " North and for longitude 4 ° 54 " West. The environment was clear and there was no shadow on the collector except the clouds between the collector and the incident rays.

B. Collector device

The collector must raise the ambient temperature (~ 27°C) to about 55°C, to provide energy to the indirect dryer to dry on 24 h about 20 kg of fermented beans. This drying time will be on 4 days. The drying is daily between 9 h and 15 h UTC, taking into account product constraints, in particular temperature and air velocity. The power produced outside the considered range will be used to compensate for deficits during bad weather.

C. Implementation of the collector

The glazing has been realized with 9 pieces of 1 m*0.5 m in order to facilitate their substitution, the thickness is 4 mm. The absorber has been made with 6 sheets of sheet metal of 2 m*0.8 m*0.5 mm in zinc and waved orthogonally to the direction of air flow. The insulation below the absorber has been built with polystyrene (2 m * 1,5 m*2 cm) and plywood sheets (2 m * 1.5 m * 1.5 cm); The lateral insulation is made of alucobond (4.7 m*15 cm * 5 mm). The other characteristics are :

M1 = 20,6 kg	Pn = 1362 W
Me = 10,63 kg	Scol = 8,2 m²
Vem = 0,43 kg/h	Lcol = 4,1 m
Xa = 16,66 g/kg	ℓcol = 2 m
Xm = 21,66 g/kg	Hcol = 0,13 m
Da = 147,67 m^3/h	

D. Apparatus

Thermo-hygrometer: Measurement of the temperature and humidity of the air inside the collector is done with an automatic data logger. Its measurement step can vary from 10 s to 12 h, corresponding to a recording, without interruption over 3 to 90 days. Its measuring range for temperature is between -35°C and 80°C, for a precision of ± 1.1 ° C. For hygrometry, the measuring range is between 0% RH and 100% RH, with a precision of 2% RH.

Anemometer: The speed and temperature of the air circulating in the collector are measured with a hot film anemometer with adjustable set measurement. The measurable velocity is between 0.2 and 20 m / s with a precision of 2% of reading.

Weather station: The measurement of the environmental parameters is carried out by a weather station, located approximately 30 m from the experimental dryer.

IV. Methods

A. Measurement procedure and experimental setup

Measurement temperature in the width of the collector: Three thermo-hygrometric probes are placed in the collector inlet at a depth of 30 cm; One is in the center about 1m from each wall, another is 20 cm from the left wall and the last is 20 cm from the right wall. They are introduced every day from 8 h to 16 h UTC in the. The values are then downloaded and only measurements of 9 h to 15 h UTC are exploited to realize averages in steps of 15 mn.

International Journal of Emerging Technology and Advanced Engineering
Website: www.ijetae.com (ISSN 2250-2459, ISO 9001:2008 Certified Journal, Volume 7, Issue 5, May 2017)

Configuration of the collector: Three holes were made in each of the 2 front legs of the collector, one at 20cm, another at 30 cm and last at 50 cm so as to place a wedge to fix the height of the inlet of the collector. In both rear legs supporting collector outlet, each 9 hole has been made corresponding of one configuration, taking into account the tilt angle and height of collector (Table 1).

TABLE 1
HEIGHT OF THE HOLES TO BE MADE ON EACH REAR FOOT AT THE OUTLET OF THE COLLECTOR IN cm

HAUTEUR / ANGLE	20 cm	30 cm	50 cm
5°	60.3	70.3	90.3
10°	100.3	110.3	130.3
15°	139.6	149.6	169.6

Determination of collector efficiency: In each configuration, the thermo-hygrometric probes are placed through the orifices made along the collector marked in red in Fig. 1, thus 2 hot-film air velocity probes are placed in the two inlet orifices (one for each channel). Measurements are recorded from 8 h to 16 h UTC in steps of 1mn. Simultaneously the radiation, the ambient temperature and the wind velocity are also measured with the same cadence.

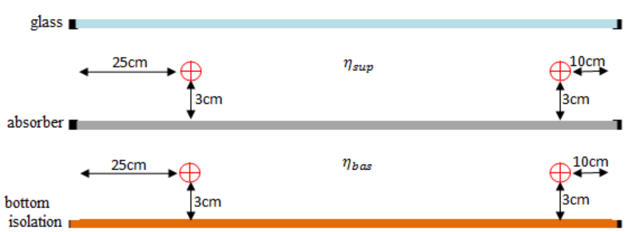

Fig. 1 Position of the thermo-hygrometric and air velocity probes in the collector (inlet and outlet) in the longitudinal direction ⊕

Statistic analyse (ANOVA) of impact of tilt angle and height of collector: The different daily values used for the efficiency calculation in each of the configurations shown in Table 4 were analyzed statistically to evaluate the influence of the angle of inclination or of the height on the thermal efficiency of the collector

D. Environmental condition during collector temperature width evaluation

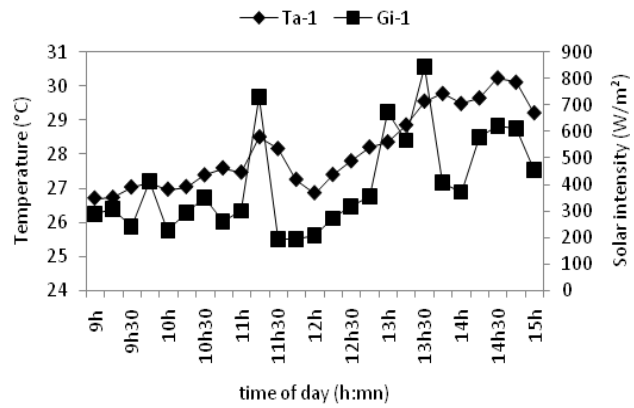

Fig. 2 Environmental condition as of 24/06/2016: (♦ Ta-1) ambient temperature, (■ Gi-1) global instantaneous radiation

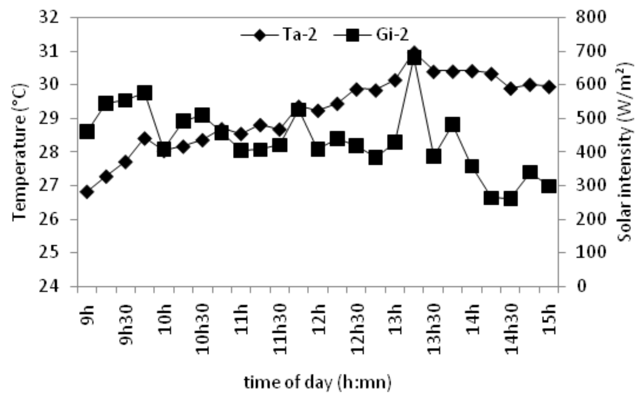

Fig. 3 Environmental condition as of 27/06/2016: (♦ Ta-2) ambient temperature, (■ Gi-2) global instantaneous radiation

Table 2
Average Of Environmental Conditions During Temperature Measurement Of The Collector Width

	Environmental conditions	
Conditions	1	2
Date	24/06/2016	27/06/2016
Time of day(UTC)	9 h-15 h	9 h-15 h
Average ambient temperature (° C)	28.2	29.3
Ambient air flow velocity (m/s)	0.833	1.816
Average solar intensity (W/m²)	408	433.6

International Journal of Emerging Technology and Advanced Engineering
Website: www.ijetae.com (ISSN 2250-2459, ISO 9001:2008 Certified Journal, Volume 7, Issue 5, May 2017)

V. Results

The experimental results are presented in form of graphs and in tables, on four parts. The first is about the impact of transversal temperature in width collector on it efficiency (A), the second is about the best configuration of collector (B) and the last is about the characteristic of the air outlet collector (C).

A. Influence of the gradient of temperature in collector width

For this part, we used 2 meteorological conditions where the thermal behaviour of collector not the same, but we stay in the same configuration.

Temperature in collector width: Fig. 4 shows during condition 1 (24/06/2016) the variation of temperature at 20 cm from the left side (● G-1), at 1 m from each side (■ C-1), at 20 cm from the right side (▲ D-1), and the average air flow velocity in inlet (♦ $V_{air\ col}$-1).

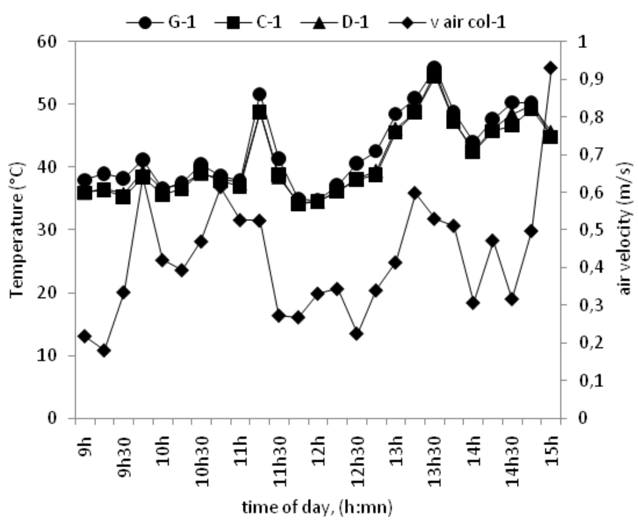

Fig. 4 Profiles in upper channel: temperature in the collector width at 30 cm from the inlet and average air flow velocity at this inlet during condition 1 (24/06/2016)

From Fig.4 and 2, it can be seen that the instantaneous solar radiation profile of 9 h to 15 h UTC is greatly identical to the variation of temperature in 3 points of the width in collector. In Fig. 4 we can be seen that before 11 h UTC the temperature oscillates between 35°C and 40°C, then there is an abrupt evolution where 50°C is practically attained, then decrease to 35°C around 11 h 45 UTC.

Later there is an increase up to 55°C at 13 h 30 UTC, then a new decrease to 44°C at 14 h UTC. Then the temperature increases but limited to 50°C at 14 h 45 UTC and decline again to 45°C around 15 h UTC. For air flow, we shows many fluctuation of velocity.

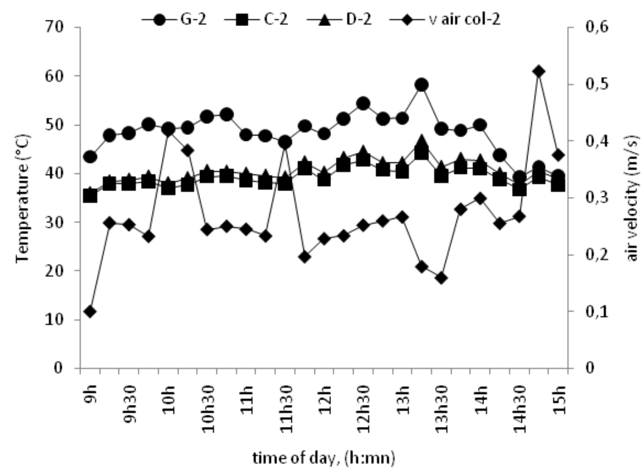

Fig. 5 Profiles in upper channel: temperature in the collector width at 30 cm from the inlet and average air flow velocity at this inlet during condition 2 (27/06/2016)

From Fig.5 and 3, it can be seen again a similarity between profile of temperature in collector width and instantaneous solar radiation. The temperature on the left is significantly higher than the other right and center with a regular gap, except from 14 h 30 UTC, but profiles is the same. The temperature on the left is growing up 43°C to 58°C from 9 h to 13 h UTC. After temperature decrease to 39°C at 14 h 30 UTC and stay around this value until 15 h UTC .

Temperature in collector length in 2 channel: Fig. 6 shows during the both condition (1 and 2) the temperature at 30 cm from inlet ($T_{e\ col}$) and 10 cm from outlet ($T_{s\ col}$). In condition 1, there is a regular gap before 11 h 30 UTC with temperatures varying between 27°C and 33°C at the inlet and between 35°C and 42°C for the outlet. In condition 2 the regular gap is continuous and the temperature growing up 27°C to 31°C at the inlet and 33°C to 38°C for the outlet.

International Journal of Emerging Technology and Advanced Engineering
Website: www.ijetae.com (ISSN 2250-2459, ISO 9001:2008 Certified Journal, Volume 7, Issue 5, May 2017)

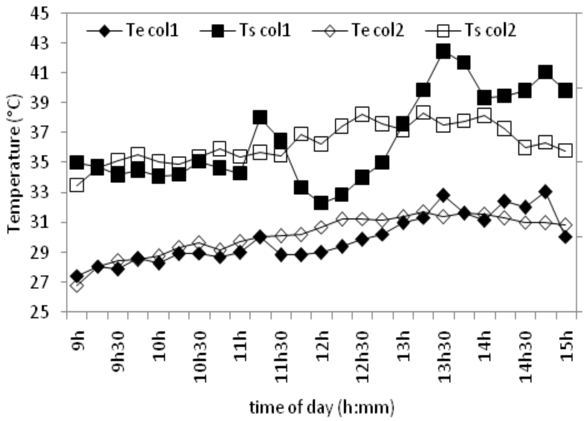

Fig. 6 Profiles of temperature in inlet and outlet of collector

Efficiency of collector in each condition: Fig. 7 shows many fluctuating, but the best efficiency is in condition 1.

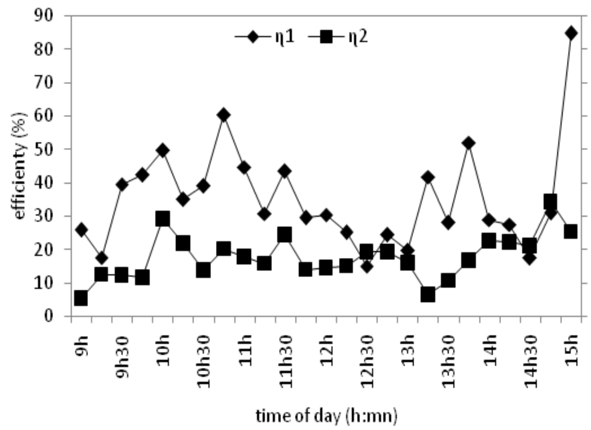

Fig. 7 Profiles of collector efficiency in condition 1 (η1) and in condition 2 (η2)

B. Influence of the positioning of the collector

All position of the collector described in Table 1 have been made. In each position, more than 4 measurements were carried out. ANOVA statistical analysis was used on these values and results are in Table 4 and 5. From Table 3, it can be seen that significance value (P=0.0004) at 15° who indicate a statistically significant difference between efficiencies. From Table 4, the significance value (P=0.00082) is at 20 cm. Furthermore, for each position, the temperature and environmental conditions were measured over 4 days, then the useful power and the efficiency were calculated. All results are in Table 5.

TABLE 3
ANOVA P-VALUE FOR EFFICIENCY WITH DIFFERENT HIGTH OF COLLECTOR IN EACH ANGLE

5°			10°			15°		
20 cm	30 cm	50 cm	20 cm	30 cm	50 cm	20 cm	30 cm	50 cm
P=0.929			P=0.110			P=0.0004		

TABLE 4
ANOVA P-VALUE FOR EFFICIENCY WITH DIFFERENT ANGLE OF COLLECTOR IN EACH H IGTH

20 cm			30 cm			50 cm		
5°	10°	15°	5°	10°	15°	5°	10°	15°
P=0.00082			P=0.017			P=0.6844		

International Journal of Emerging Technology and Advanced Engineering
Website: www.ijetae.com (ISSN 2250-2459, ISO 9001:2008 Certified Journal, Volume 7, Issue 5, May 2017)

TABLE 5
AVERAGE VALUES IN EACH CONFIGURATION BETWEEN 9 H AND 15 H UTC

	Average values								
α (°)	5°			10°			15°		
h (cm)	20	30	50	20	30	50	20	30	50
Te col (°C)	34.71	35.15	32.97	32.55	32.34	32.03	32.75	32.39	32.61
Ts col (°C)	40.43	41.78	39.34	38.74	38.37	38.12	44.42	45.95	44.45
Ta moy (°C)	32.52	33.64	31.69	31.24	30.56	29.93	30.31	30.40	30.96
ΔT col (°C)	5.71	6.63	6.37	6.19	6.03	6.09	11.67	13.56	11.84
v air (m/s)	1.68	1.75	1.67	1.61	1.39	1.21	1.21	1.17	1.29
Gi (W/m²)	664.84	682.80	587.87	540.63	562.64	597.92	577.30	626.25	643.10
v air col (m/s)	0.55	0.45	0.45	0.43	0.46	0.48	0.39	0.24	0.30
P (W)	1210.50	1076.57	1016.61	954.83	1093.82	1160.10	1686.81	1090.33	1120.99
η (%)	23.27	22.53	23.79	24.46	32.13	26.76	39.96	23.64	25.09

The instantaneous solar radiation is average greater than 500W / m² for all configurations. We show also the temperatures at the inlet of collector are generally at 32°C, except during the first two measurements (5°-20 cm and 5°-30 cm) where they are 35°C. For outlet, the highest temperatures were recorded at 15° with a maximum of 13.56°C to 30 cm.

The air flow velocities inside the collector are averaged 0.4 m/s, but in 15° configuration the lowest is 0.24 m/s for 30 cm and the highest is 0.39 for 20 cm. The ratio of ambient wind in the collector is between 20% (15°-30 cm) and 39% (10°-50 cm). The highest power (1686 W) on average between 9 h and 15 h UTC was obtained during the 15°-20 cm configuration.

C. Thermal performance of the collector in optimum configuration (15°-20 cm) on 14/11/2016

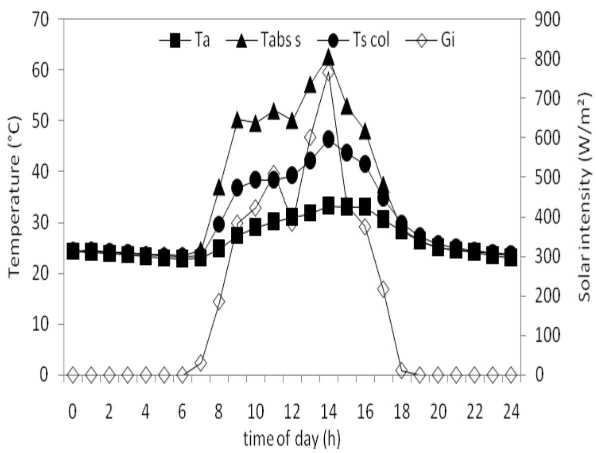

Fig. 8 Profiles of temperatures out and in the collector and global instantaneous radiation

Fig. 8 shows the variation of temperature ambient (■ Ta), absorber outlet temperature (▲ T abs s), temperature of outlet air flow (●Ts col) and solar global instantaneous radiation (◊ Gi). Between 8 h and 19 h UTC a parabolic profile is observed, for absorber temperature the maximum is 62°C to 14 h UTC, for outlet of the collector we recorded 46°C at the same time and for the ambient maximum the value is 33°C. The radiation stayed above 500 W/m² only between 13 h and 14 h UTC, its maximum value also at 14 h UTC is 766 W/m². After the temperature, air humidity is important for drying. It is therefore useful to see his course on one day.

Fig. 9 Profiles of air humidity ambient and outlet the collector

Fig. 9 shows the variation of humidity of air ambient (■ HR%) and absorber outlet (▲ HR% s col). Both are the same profile, but the value outlet of collector is always lower. Between 8 h and 19 h UTC in outlet of collector the values are less than 80%, with the lowest value (34%) around 14 h UTC. For ambient air this value (80%) is between 11 h and 18 h UTC and the minimum is 62% at 14 h UTC.

Hygrometry is associated with the proportion of water contained in the air, knowledge of the mass of water in the air at the outlet of the collector makes it possible to know the quantity of water that the air coming out of the collector will be possible to transport out the dryer.

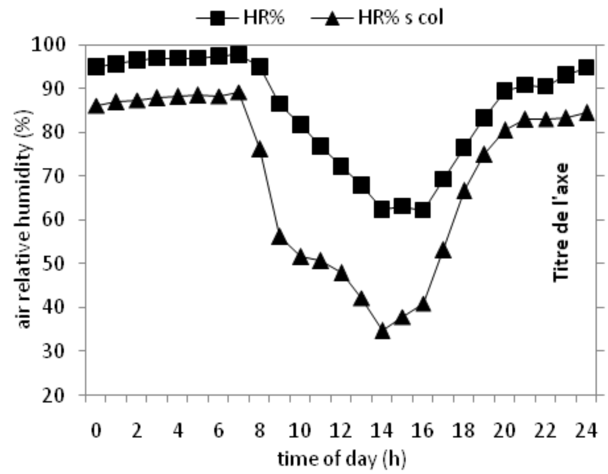

Fig. 10 Profiles of the mass of water vapour in 1 kg of dry air for ambient and outlet the collector

Fig. 10 shows the variation of mass of water vapor in air ambient (■ Wa) and absorber outlet (▲ W s col). The evolution profile is the same, practically constant (~ 42 g / kg for ambient air and ~ 18 g/kg for collector) except between 8 h and 20 h UTC where values decrease. A minimum of ~ 30 g/kg is observed at around 15h UTC for ambient air and a minimum of ~ 11 g/kg around 14h UTC for the collector outlet.

VI. Discussion

A. Impact of the transverse gradient of the temperature in the collector on the thermal efficiency

The multiple fluctuations are probably caused by clouds, which at times, reduce the intensity of the solar radiation by constituting an obstacle between the radiation and the collector. The almost simultaneous evolutions between the evolution of the global instantaneous radiation and the temperatures in the collector indicate that the radiation has a direct impact on the energy produced by it. Indeed, part of this thermal energy is absorbed by the steel sheet and communicated to the flow of air inside the collector and another part is lost. In condition 1, the left of the collector is warmer than the center and the right, probably caused by the surplus of energy which moves laterally [15] when air flow are low. Indeed, the circulation of the air flow makes it possible to carry the energy already absorbed by the collector and allow it to continue to absorb the energy.

International Journal of Emerging Technology and Advanced Engineering
Website: www.ijetae.com (ISSN 2250-2459, ISO 9001:2008 Certified Journal, Volume 7, Issue 5, May 2017)

In condition 2 the gap is more important at left temperature, probably because of the air flow velocity in the collector which is less than in condition 1. The best efficiency obtained in the latter condition can be explained by the smaller losses permitted by the better airflow. Similar results were also found by Karsli [8]. The bad recovery of the energy of the absorber by the air flow is mainly the basis of the non-homogeneity of the temperature in the width of the collector and therefore of the low efficiency.

B. Impact of the inclination of the collector and its relative height on the ground on its efficiency

P-value 0.0004 concluded that when we are at 15°, the height of collector have an impact on collector efficiency value. And P-value 0.00082 concluded that when we are at 20 cm, the angle of collector have an impact on efficiency value. Other measurements at 15 cm and 25 cm will be permit to have more information about optimal position. For the inclination of 15° of the collector, the temperature at its outlet is better, because in this configuration a maximum of incident ray probably arrive orthogonally to the collector [16]. Indeed the zones with low latitude like in our case (latitude 6°N, Côte d'Ivoire-M'birmbo) the optimum angle of inclination is between 5 and 16° [17]. Moreover, in this same inclination, the differences of temperatures are explained more by the difference in airflow velocity than by the difference in radiation.

C. Thermal behavior at the outlet of the collector in its optimal configuration

Temperatures between 9 h and 16 h UTC are limited to 46 ° C, probably because the absorber is not painted in black to maximize the absorption of energy. This limited temperature has no fatal incidence on cocoa beans during a drying in these conditions. Indeed at temperatures above 55°C the proportion of antioxidant contained in the bean decreases rapidly [18], [19], moreover, the water is extracted more quickly from the bean than the contained acidity [20], thus influencing negatively the taste quality of the beans. With an average hygrometry of 46 % between 9 h and 16 h UTC, this air cannot entrain the crusting of the surface of cocoa beans [6]. The air flow velocity at the collector outlet varying around 0.4 m/s is well within the ideal range for drying cocoa [21]. The small amount of water vapor in the air at the outlet of the collector (~ 13g/kg) relative to that of the ambient air (35.75g/kg), allows the drying air to carry more water.

VII. Conclusion

The solar collector who can produce the energy useful to dry 20 kg of cocoa beans has been successfully realized and tested in this study. Results obtained permit to concluded that a low air flow and too much air flow in collector decreases the efficiency. The height of the collector can affect the efficiency of the output when the optimum angle is determined. The characteristics of the air at the outlet of the collector make it possible to offer controlled drying to cocoa beans.

Acknowledgement

We would like to thank the State of Côte d'Ivoire for financing by the PreSeD-Ci and AMRUGE-CI projects under the debt reduction contract, as well as the IRD and the France embassy in Côte d'Ivoire for the management of the financing obtained. At the same time, we would like to thank the SAB for the working site.

REFERENCES

[1] M. Torres-Moreno, E. Torrescasana, J. Salas-Salvadó, and C. Blanch, "Nutritional composition and fatty acids profile in cocoa beans and chocolates with different geographical origin and processing conditions," Food Chem., vol. 166, pp. 125–132, 2015.

[2] N. Camu, T. De Winter, S. K. Addo, J. S. Takrama, H. Bernaert, and L. De Vuyst, "Fermentation of cocoa beans: influence of microbial activities and polyphenol concentrations on the flavour of chocolate," J. Sci. Food Agric., vol. 88, no. 13, pp. 2288–2297, 2008.

[3] J.-F. Rozis, Drying of agricultural products. Techniques, procedures, equipment. Groupe de Recherches et d'Échanges Technologiques (GRET), 1995.

[4] C. Law, H. Chen, and A. Mujumdar, "Food technologies: drying," Encycl. Food Saf., vol. 3, pp. 156–167, 2014.

[5] B. J. Kouakou, B. Z. Irie, E. Dick, G. Nemlin, and L. E. Bomisso, "Caractérisation des techniques de séchage du cacao dans les principales zones de production en Côte d�Ivoire et détermination de leur influence sur la qualité des fèves commercialisées," J. Appl. Biosci., vol. 64, no. 1, pp. 4797–4812, 2013.

[6] F. Augier, "Transport d'eau et d'acide en milieu complexe. Application au séchage de la fève de cacao," Montpellier 2, 1999.

[7] I. Ohijeagbon, L. Ogunforowa, J. Omale, and P. Ameh, "Energetic performance analysis of drying agricultural products integrated with solar tracking," Niger. J. Technol., vol. 35, no. 4, pp. 825–830, 2016.

[8] S. Karsli, "Performance analysis of new-design solar air collectors for drying applications," Renew. Energy, vol. 32, no. 10, pp. 1645–1660, 2007.

[9] C. A. Djedjro, N. E. Assidjo, and B. Yao, "Effets des dispositifs de sechage a l' air libre sur la qualite des feves de cacao bord champ," pp. 45–58, 2008.

[10] P. García-Alamilla, M. Salgado-Cervantes, M. Barel, G. Berthomieu, G. Rodriguez-Jimenes, and M. García-Alvarado, "Moisture, acidity and temperature evolution during cacao drying," J. Food Eng., vol. 79, no. 4, pp. 1159–1165, 2007.

[11] J.-P. Nadeau and J.-R. Puiggali, "Séchage: des processus physiques aux procédés industriels," 1995.

[12] Y. Jannot, thermique Solaire. 2011.

[13] A. Zerrouki, B. Tedjiza, and N. Said, "Modélisation des Pertes Thermiques dans un capteur Solaire à Air à deux Passes," Rev. Energ. Renouvelables, vol. 5, no. 5, pp. 49–58, 2002.

[14] K. Ong, "Thermal performance of solar air heaters: mathematical model and solution procedure," Sol. Energy, vol. 55, no. 2, pp. 93–109, 1995.

[15] U. Eicker, Solar technologies for buildings. John Wiley & Sons, 2006.

[16] E. A. Handoyo, D. Ichsani, and others, "The optimal tilt angle of a solar collector," Energy Procedia, vol. 32, pp. 166–175, 2013.

[17] C. Oko and S. Nnamchi, "Optimum collector tilt angles for low latitudes," Open Renew. Energy J., vol. 5, pp. 7–14, 2012.

[18] J. Alean, F. Chejne, and B. Rojano, "Degradation of polyphenols during the cocoa drying process," J. Food Eng., vol. 189, pp. 99–105, 2016.

[19] T. M. Kyi, W. R. W. Daud, A. B. Mohammad, M. Wahid Samsudin, A. A. H. Kadhum, and M. Z. M. Talib, "The kinetics of polyphenol degradation during the drying of Malaysian cocoa beans," Int. J. Food Sci. Technol., vol. 40, no. 3, pp. 323–331, 2005.

[20] D. Páramo, P. García-Alamilla, M. Salgado-Cervantes, V. Robles-Olvera, G. Rodríguez-Jimenes, and M. García-Alvarado, "Mass transfer of water and volatile fatty acids in cocoa beans during drying," J. Food Eng., vol. 99, no. 3, pp. 276–283, 2010.

[21] M. Krokida, E. Foundoukidis, and Z. Maroulis, "Drying constant: literature data compilation for foodstuffs," J. Food Eng., vol. 61, no. 3, pp. 321–330, 2004.